

# Grain Refinement under Multiple Warm Deformation in 304 Type Austenitic Stainless Steel

A. BELYAKOV,<sup>1,2)</sup> T. SAKAI,<sup>1)</sup> H. MIURA<sup>1)</sup> and R. KAIBYSHEV<sup>2)</sup>

1) Department of Mechanical Engineering and Intelligent Systems, The University of Electro-Communications, Chofu, Tokyo 182-8585, Japan. 2) Institute for Metals Superplasticity Problems, Ufa 450001, Russia.

(Received on November 25, 1998; accepted in final form on March 5, 1999)

The dynamic process of fine grain evolution as well as deformation behaviour under warm working conditions was studied in compression of a 304 type austenitic stainless steel. Multiple compression tests were carried out at a strain rate of  $10^{-3} \text{ s}^{-1}$  to produce high cumulative strains, with changing of the loading direction in  $90^\circ$  and decreasing temperature from 1 223 to 873 K ( $0.7\text{--}0.57T_m$ ) in each pass. The steel exhibits two types of deformation behaviours with different mechanical and structural characteristics. In the deformation region where flow stresses are below about 400 MPa, conventional dynamic recrystallization takes place accompanied mainly by bulging of serrated grain boundaries. The dynamic grain size evolved can be related to the high temperature flow stress through a power law function with a grain size exponent of  $-0.72$ . On the other hand, in the region of higher stresses above 400 MPa the flow stresses show small strain rate and temperature dependence, and so it is suggested to be in an athermal deformation region. The stress-strain curves show a steady state like flow without any strain softening, while the multiple deformation to high cumulative strains brings about the evolution of fine grained structures with grain sizes less than one micron. The relationship between the warm temperature flow stresses and the grain sizes evolved also can be expressed by a unique power law function of grain size with an exponent of  $-0.42$ . The interrelations between the mechanisms of plastic deformation and microstructure evolution at warm and high temperatures are analysed in detail and also the multiple compression method for obtaining ultra fine grained structure is discussed as a simple thermomechanical processing.

**KEY WORDS:** austenitic stainless steel; multiple warm deformation; conventional and continuous dynamic recrystallization; strain-induced grain refinement; nanoscale grains.

## 1. Introduction

Grain refinement in metals and alloys through hot working is of great practical importance because of several improved properties of the material products. Extensive investigations have demonstrated that the considerable refinement of microstructure can be achieved by imposing very high cold and/or warm plastic deformations.<sup>1-6)</sup> One of difficulties for their scientific analyses and also industrial application is limited to the workability or ductility of many metals and alloys at low to moderate temperatures. Several techniques have been proposed to produce such severe high strains, *e.g.* torsion under high pressure<sup>1-5,7)</sup> and equal channel angular pressing.<sup>2,5,6)</sup> These methods, however, have some limitations for their widespread use in industry because of the high working power for work-hardened sizeable products and the calculation of true deformation parameters, *e.g.* stress and strain, comparable with the other processes. An another technique is multiple forging, which can lead to the submicrocrystalline structure formation in various materials at moderate temperatures.<sup>2,5)</sup>

Several mechanisms operating under such strain in-

duced grain refinement are proposed in previous studies.<sup>3,4,6-14)</sup> It is shown in them that the new grain formation taking place at low temperatures follows the evolution of deformation induced subboundaries in grain interiors.<sup>3,4,6,12-14)</sup> The latter's misorientations are increased by the accumulation of dislocations at subboundaries and/or subgrain rotation at high strains, leading to the formation of fine grains assisted by dynamic recovery (DRV). An another important mechanism for the microstructure formation taking place under hot deformation is the conventional dynamic recrystallization (DRX), which usually takes place in many materials with low to medium stacking fault energies.<sup>8-11)</sup> The characteristics of DRX, such as the dynamic grain sizes, their dependence on deformation conditions and the effect of initial microstructure on DRX behaviour, have been fairly clarified under hot deformation condition. The DRX grain sizes evolved sensitively decrease with temperature decreasing or with strain rate increasing. Such dependence for DRX grain size can lead to the formation of much finer grained structures under cold or warm working. It is generally agreed that there will be a critical deformation condition for DRX occurrence,<sup>14-17)</sup> although the decrease

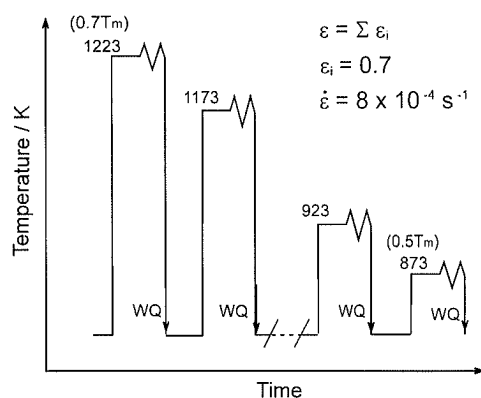


**Fig. 1.** Schematic diagram of the thermomechanical processing method used in multiple compression with continuous decreasing temperature in each pass. The loading direction is changed in 90° with pass-to-pass.

in initial grain size may accelerate DRX kinetics.

The aim of the present work is to study the strain induced microstructure evolution in an austenitic stainless steel during multiple compression with continuous decrease in temperature from hot to warm deformation. This work is also aimed to clarify any limit for the occurrence of conventional DRX and the effects of deformation conditions and initial microstructure on the interrelation between deformation behaviours and structural changes. A 304 austenitic stainless steel was used as one of the typical commercial-base materials showing conventional DRX behaviour under hot working.<sup>17)</sup>

## 2. Experimental Procedure

A 304 type austenitic stainless steel (0.058% C, 0.7% Si, 0.95% Mn, 0.029% P, 0.008% S, 8.35% Ni, 18.09% Cr, 0.15% Cu, 0.13% Mo and the balance Fe) with an initial grain size of about 25  $\mu\text{m}$  was used as the samples for compression tests. **Figure 1** represents a schematic diagram for the present thermomechanical processing method used. The rectangular samples with a starting dimension of 10 × 10 × 13 mm were machined for multiple compression tests. The tests were carried out with changing of the loading direction in 90° with pass-to-pass, *i.e.* samples were rotated in order of three perpendicular axes (*i.e.*  $x$  to  $y$  to  $z$  to  $x \cdots$ ). After each step of deformation the specimens were repeatedly machined and/or ground to right-angle shape. The starting temperature of 1223 K (0.7T<sub>m</sub>) continuously decreased in 50 K at each deformation pass, and finally approached 873 K (0.5T<sub>m</sub>). The samples were compressed in vacuum with a powder of boron nitride as a lubricant under a strain rate of  $8 \times 10^{-4} \text{ s}^{-1}$ . The tester enabling a true strain rate constant was equipped with a water quenching apparatus.<sup>18)</sup> The true strains applied in each deformation pass were  $0.7 \pm 0.05$  and the cumulative strains after various numbers of passes were calculated by summation of prior strains in each pass. The period of preheating time before recompression was about 0.6–0.9 ks. The metallographic analysis was carried out on the sections parallel to the compression

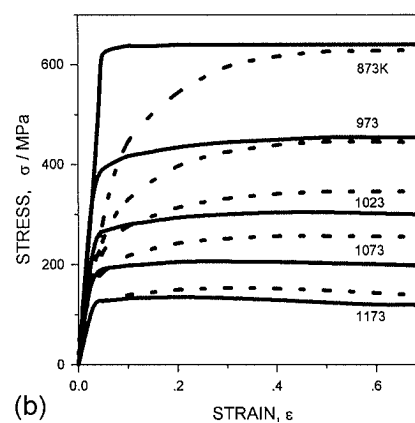
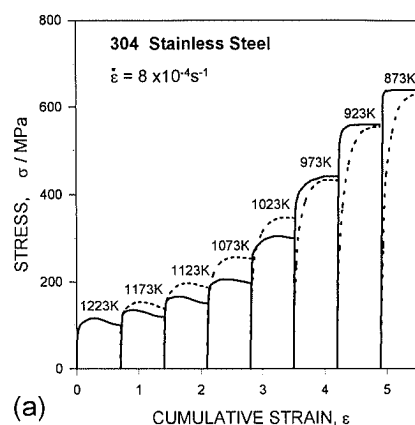


**Fig. 2.** (a) A series of true stress–strain ( $\sigma$ – $\epsilon$ ) curves (solid lines) for a 304 stainless steel under multiple compression with temperature decreasing from 1223 to 873 K at  $8 \times 10^{-4} \text{ s}^{-1}$ . Dashed lines indicate  $\sigma$ – $\epsilon$  curves for usual single-pass compression of initially annealed samples.<sup>16)</sup> (b) Some magnified  $\sigma$ – $\epsilon$  curves in both of the testing methods.

axis of deformed samples using an Olympus PME3 optical microscope and the dislocation substructures were examined in a JEM-2000FX transmission electron microscope (TEM). The misorientations on grain boundaries and subboundaries were studied using a conventional Kikuchi-line technique.<sup>19)</sup> The accuracy of calculations was about one degree because of high dislocation densities evolved. The experimental results obtained in the present work are compared with those obtained under usual single-pass compression of the same material.<sup>17)</sup>

## 3. Experimental Results

### 3.1. Multiple Deformation Behaviour

A series of the stress–strain ( $\sigma$ – $\epsilon$ ) curves under multiple compression tests with temperature decreasing from 1223 to 873 K is shown in **Fig. 2**. Dashed lines in this figure show the single-pass compression flow curves of the annealed 304 steel at the same range of temperatures and at a strain rate of  $8 \times 10^{-4} \text{ s}^{-1}$ .<sup>17)</sup> It is remarkably noted in **Fig. 2** that flow stresses at moderate strains for annealed samples are higher than those for pre-deformed ones, *i.e.* under multiple compression, at temperatures above 1023 K, while they become conversely lower at

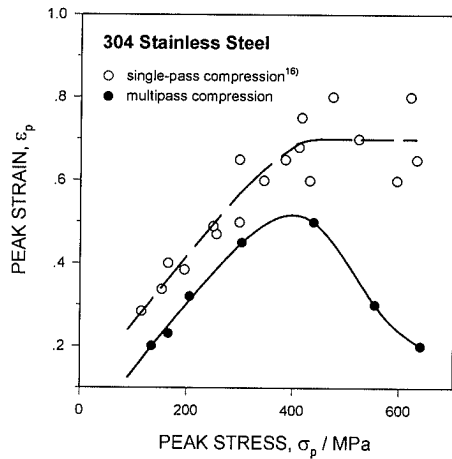


**Fig. 3.** Relationship between the stress ( $\sigma_p$ ) and the strain ( $\epsilon_p$ ) where a peak appears in the flow curves for a 304 stainless steel. In the case of steady state flow under multi-pass deformation, the steady state flow stress and its beginning strain are plotted as  $\sigma_p$  and  $\epsilon_p$ , respectively.

the temperatures of below 973 K. At temperatures of  $T \geq 1023$  K (or at flow stresses below around 400 MPa), the flow stresses for pre-deformed samples rapidly increase to a peak followed by a strain softening for each deformation pass. Such flow behaviours appear accompanied by typical DRX taking place under hot working.<sup>8-11,16,17</sup> It should be noted in Fig. 2 that the  $\sigma$ - $\epsilon$  curves under multiple tests rapidly approach a steady-state flow following a strain softening at lower strains, as compared to those for annealed samples. As shown in some previous works,<sup>8,9,14,20</sup> this can be because DRX rapidly takes place in the former due to strain accumulation, leading to the appearance of lower flow stresses. On the other hand, any strain softening does not appear during deformation at temperatures below 973 K. In this deformation region, where the flow stresses are above around 400 MPa, the flow stresses approach a saturation value at high strains and so the  $\sigma$ - $\epsilon$  curves show steady-state-like flows. The steady-state flow stresses in each pass are larger at moderate strains, but almost the same at high strains comparing with the stresses under single-pass compression. The yield stresses in each pass should be affected by static recovery and/or recrystallization taking place for a period of reheating time. Figure 2 suggests that such a static annealing effect appears quite small under interrupted tests at temperatures below 973 K. A steady-state-like flow appears in the region of warm deformation, where the general shape of the  $\sigma$ - $\epsilon$  curves is similar to that controlled by dynamic recovery (DRV).<sup>8,11,14</sup>

The relationship between the peak stress ( $\sigma_p$ ) and the corresponding peak strain ( $\epsilon_p$ ) is shown in Fig. 3.\* The  $\epsilon_p$  increases with  $\sigma_p$  in the region of  $\sigma_p < 400$  MPa. This is similar to the results for single-pass compression of annealed samples, although the  $\epsilon_p$  in multi-pass condition is always smaller against the same values of  $\sigma_p$ . On the other hand, the  $\epsilon_p$  rapidly decreases with increase in  $\sigma_p$  in the region of  $\sigma_p > 400$  MPa, while that for annealed

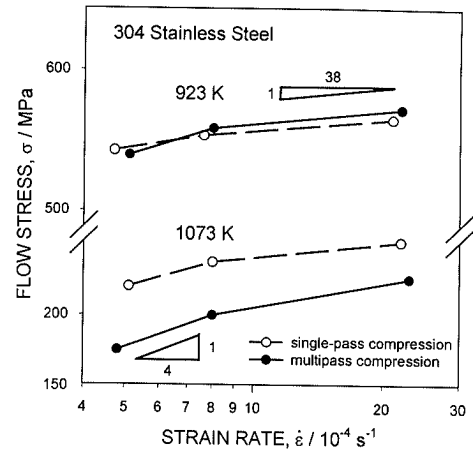


**Fig. 4.** Relationship between flow stress and strain rate for a 304 stainless steel tested by strain rate changing instantaneously at a strain of 0.65 above peak strain. The slope indicates the stress exponent in power law equation, namely  $n = (\Delta \ln \dot{\epsilon}) / (\Delta \ln \sigma)$ .

samples are roughly constant.

To study the strain rate dependence of flow stress under multiple compression, an initial strain rate of  $8 \times 10^{-4} \text{ s}^{-1}$  was instantaneously increased or decreased at a strain of 0.65 at 923 and 1073 K. Figure 4 shows the strain rate dependence of flow stress plotted in double logarithmic scale. The data for annealed samples under single-pass compression<sup>17</sup>) also are included for comparison. It can be seen in Fig. 4 that a high strain rate dependence of flow stress at 1073 K dramatically changes to a quite weak dependence, namely the stress exponent ( $n$ ) of 4 to 7 at 1073 K rapidly increases to above 38 at 923 K. These results in multi-pass deformation are roughly the same as those in single-pass one, although the strain rate sensitivities in the former are a bit higher compared with those in the latter. It can be concluded from Fig. 4, therefore, that the temperatures used in the present study are in a transient region from athermal to thermal deformation.

### 3.2. Structure Evolution under Multiple Deformation

A main feature of structural changes during multiple deformation is a grain refinement taking place at all of the testing conditions, as shown in Figs. 5 and 6. At temperatures above 1023 K the microstructures evolved under multi-pass deformation are similar to those developed by single-pass compression.<sup>17</sup>) Further decreasing temperature to below 1000 K, no fine grains were evolved in pan-caked original grains under single-pass compression to a strain above one.<sup>17</sup>) It can be clearly seen in Fig. 6, in contrast, that fine grain evolution takes place even at  $0.5T_m$ , i.e. 873 K, under multiple deformation. The volume fraction of such fine grained structure in Fig. 6a is about 45%. The other type of microstructure evolved under multiple deformation at 873 K, as shown in Fig. 6b, is very high density dislocation substructures including dense dislocation walls (DDWs). This is similar to the substructures developed under cold deformation.<sup>21,22</sup>)

\* The steady-state flow stress and its beginning strain are plotted as  $\sigma_p$  and  $\epsilon_p$  at lower temperatures, where no strain softening takes place.

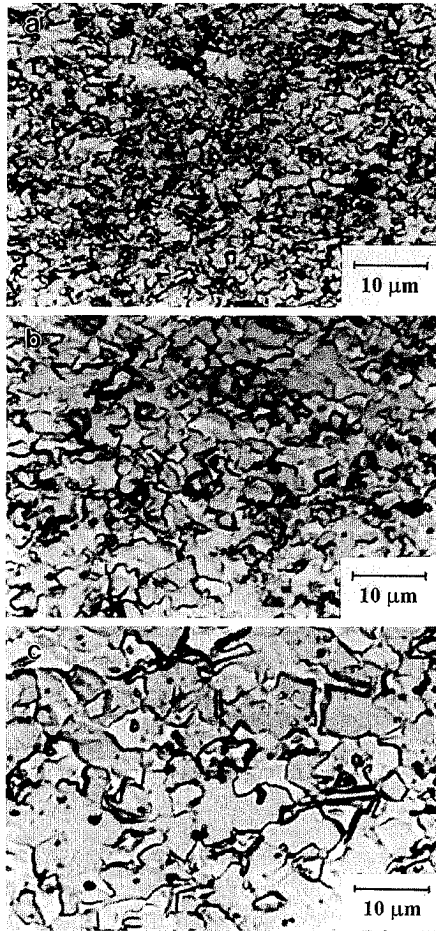


Fig. 5. Microstructures developed under multiple compression of a 304 stainless steel at various accumulated high strains ( $\Sigma\epsilon$ ) and last pass temperatures ( $T$ ). (a)  $\Sigma\epsilon=3.5$ ,  $T=1023$  K, (b)  $\Sigma\epsilon=2.8$ ,  $T=1073$  K and (c)  $\Sigma\epsilon=1.4$ ,  $T=1173$  K.

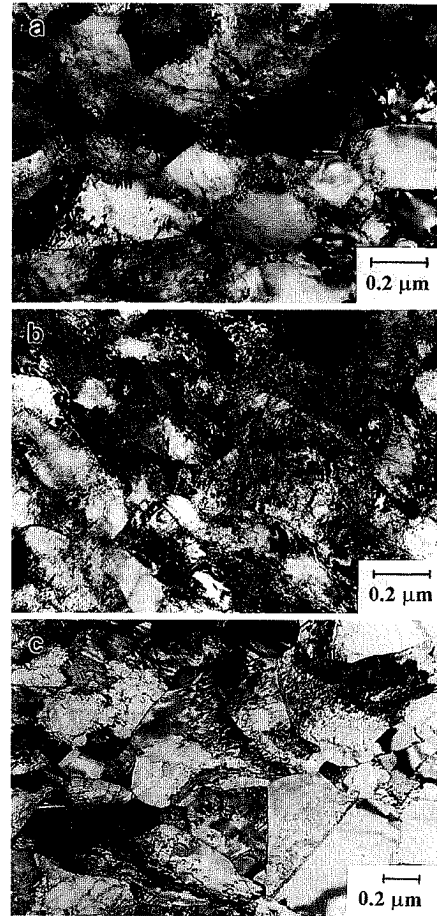


Fig. 6. Effect of temperature and accumulated strain on microstructures evolved under multi-pass compression of a 304 stainless steel. (a) and (b)  $\Sigma\epsilon=5.6$ ,  $T=873$  K and (c)  $\Sigma\epsilon=4.2$ ,  $T=973$  K.

The dynamic grain sizes evolved decrease with decrease in deformation temperature\* (or increase in strain rate), as can be seen in Figs. 5 and 6. It is well known that a unique power law relationship between flow stress ( $\sigma$ ) and dynamic grain size ( $D$ ) generally holds for various DRX-type materials<sup>8-11,16,17</sup> and can be represented by a following equation:

$$\sigma = K_1 D^{-N} \dots\dots\dots(1)$$

where  $K_1$  and  $N$  are experimental constants. The exponent  $N$  usually lies in the range from 0.7 to 0.8 for most single-phase materials.<sup>8-11,16,17</sup> The relationship between average grain size, evaluated by both optical microscopy and TEM, and the peak flow stress is represented in Fig. 7 in log-log scale. Figure 7 also includes the data obtained by optical microscopy in single-pass compression.<sup>17</sup> It can be seen in Fig. 7 that the data on  $\sigma_p$  and  $D$  are almost the same within an experimental scatter irrespective of multi-pass and single-pass deformation as well as the evaluation of optical microscopy and TEM. The  $\sigma_p$  vs.  $D$  relationship can be approximately represented by Eq. (1) even under submicron scale grains, while it changes in the two domains to be distin-

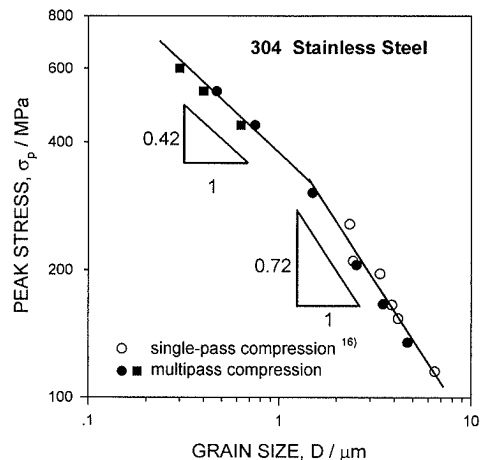


Fig. 7. Relationship between peak flow stress and dynamic grain size under multiple deformation (closed marks) of a 304 stainless steel. The circles and squares indicate the grain sizes evaluated by light microscopy and TEM, respectively. The data for single-pass compression (open marks) are included for comparison.<sup>16)</sup>

guished at a critical stress of 300–400 MPa. The grain size exponent, *i.e.* the slope, is  $-0.72$  in the region below 350 MPa, *i.e.* under hot deformation. On the other

\* Here deformation temperature means the temperature for a last pass in multi-pass compression.

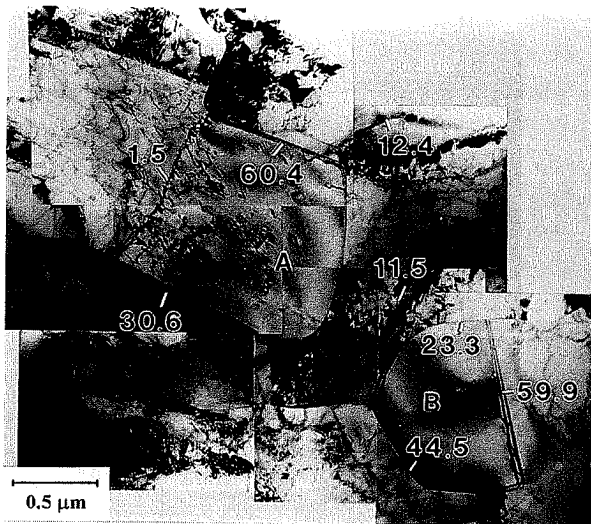


Fig. 8. TEM micrograph of fine structure evolved by multiple hot deformation in last pass at 1073 K ( $\Sigma\varepsilon=2.8$ ). Note several new grains evolved towards a grain interiors with high density dislocations in a 304 stainless steel.

hand, the  $N$  in the region of warm deformation is 0.42, which is clearly different from 0.72 in hot deformation. Note here that this critical stress of around 350 MPa is roughly similar to that about 400 MPa for deformation behaviour in Fig. 2 or 3.

Let us consider the characteristics of microstructure evolution in some more detail. Figure 8 shows a typical TEM micrograph of fine grained structure developed under multi-pass compression at a temperature of 1073 K, which is in the region of hot working. It can be clearly seen in Fig. 8 that microregions with high misorientations include high and low dislocation densities, which can correspond to work hardening and softening. Such structural heterogeneity is one of main characteristics of conventional DRX, wherein new grains can dynamically nucleate and grow in deformed matrix.<sup>23)</sup> Two microregions with moderate dislocation densities can be as nuclei for new grains, lettered by A and B in Fig. 8. These nuclei may be evolved as a result of local migration of their boundaries toward the surrounding regions with high dislocation densities. This strongly suggests that the bulging of grain boundaries can be a mechanism of new grain formation under hot deformation, as discussed in detail in previous papers.<sup>17,24,25)</sup> Another important point to be noted is a role of strain induced dislocation subboundaries and twinning on the new grain formation. The nuclei of A and B containing low dislocation densities are separated from their parent grains by a low angle dislocation subboundary and a twin boundary, respectively. Dynamic new grains, therefore, are frequently evolved with the formation of strain induced dislocation subboundaries. These are special features of dynamic nucleation by bulging mechanism.<sup>17)</sup> The microstructural heterogeneities inherent in DRX substructures are also developed in warm multi-pass deformation, as can be seen in Fig. 6. The new grains with low to high dislocation densities in Fig. 6a suggest that any restoration processes except DRX may take place in highly strained

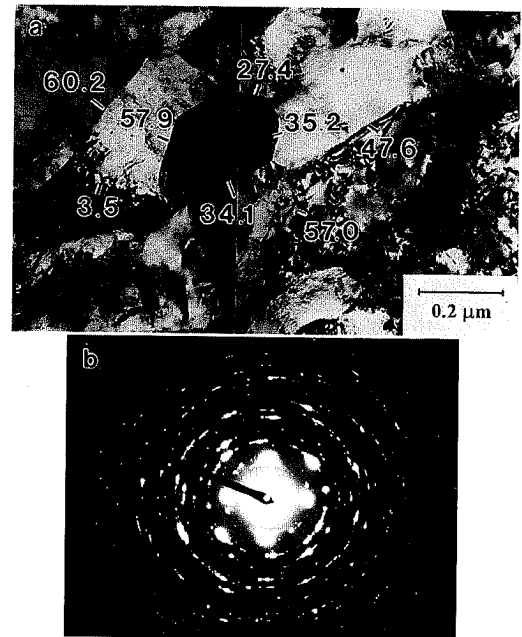


Fig. 9. Typical TEM micrograph and diffraction pattern of microstructure evolved in a final pass at 873 K for a 304 stainless steel by multiple warm deformation to  $\Sigma\varepsilon=5.6$ . Many spots circle-like microdiffraction in (b) was obtained from selected area of 2  $\mu\text{m}$  in diameter.

matrices at warm temperatures.

Figure 9 shows another typical example of fine grained region evolved under warm multiple deformation at a last pass temperature of 873 K. The analysis of orientation for several fine grains in Fig. 9a can reveal that this microstructure is composed of many fine grains with high angle boundaries, where dislocation substructures in grains are more recovered. This can be supported by many spots circle-like microdiffraction pattern in Fig. 9b, which was obtained from a selected area of 2  $\mu\text{m}$  in diameter. It should also be noted that the diffuse character of the diffraction spots in Fig. 9b can indicate high lattice curvatures and so some internal stresses developed in these fine grains.

## 4. Discussion

### 4.1. Conventional DRX under Multiple Deformation

It has been shown in the previous study for the 304 stainless steel<sup>17)</sup> that the deformation characteristics appearing in the temperatures from 0.5 to 0.7 $T_m$  cover those under warm and hot deformation. The transition takes place roughly at a deformation condition where flow stresses become around 400 MPa under single-pass compression and this is also confirmed by the present multiple deformation. It can be reasonable that such a change in flow behaviours from warm to hot deformation should influence some characteristics of dynamic structure evolution.

Under hot deformation where flow stresses are below 400 MPa, the flow behaviour and related microstructure development in 304 stainless steel are affected by conventional DRX. In the present study, the initial grain sizes in each multi-pass compression should depend on

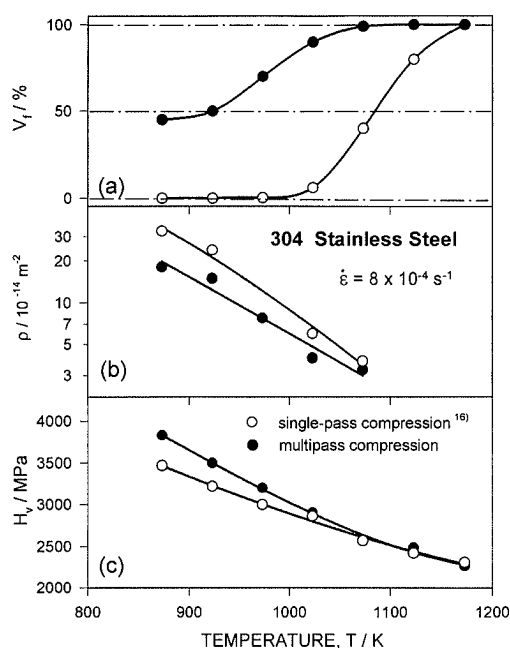


Fig. 10. Effect of deformation temperature ( $T$ ) on (a) volume fraction of new grains ( $V_f$ ), (b) average dislocation density ( $\rho$ ) and (c) room temperature hardness ( $H_v$ ) for single-pass<sup>16)</sup> and multi-pass compression of 304 stainless steel.

the preceding deformation. The development of smaller grain sizes as well as heterogeneous dislocation substructures under multiple deformation<sup>20)</sup> can result in the rapid development of new DRX microstructures as well as lower flow stresses, as shown in Figs. 2 and 3. This also is confirmed in Fig. 10(a) that a full development of DRX grains takes place at 1023 K under multi-pass deformation, while that occurs at 1173 K during single-pass one.

It has been discussed<sup>10,11,17,24,25)</sup> that the dynamic nucleation under hot working conditions frequently takes place by bulging of serrated grain boundaries. This is again supported by Fig. 8. The nuclei of new grains (A and B in Fig. 8) appearing due to local grain boundary migration are frequently separated from the parent grains by the formation of strain induced low to middle angle dislocation subboundaries and some times twins, as can be seen in Fig. 8. The misorientations of such dislocation boundaries are increased by further straining accompanied with DRV, finally leading to the evolution of conventional grain boundaries with high misorientations.<sup>17,25)</sup> A possible mechanism of increase in boundary misorientations may be an occurrence of grain rotations accompanied by grain boundary sliding or shearing.<sup>17,24,25)</sup>

#### 4.2. Grain Refinement at $0.5T_m$

Under warm deformation where flow stresses are above 400 MPa, the  $\sigma$ - $\epsilon$  curves show steady-state-like flows. The flow stresses at high strains are almost similar under both single-pass and multi-pass compression in Fig. 2, while the evolution of new grains takes place only after multiple deformation is carried out. It is generally agreed that DRV can control the flow behaviours in the athermal region, but does not lead to a new grain evolution at

moderate strains. In present study the effect of strain accumulation under multi-pass warm compressions becomes very important for the evolution of dislocation substructures as well as new grains, and so the grain refinement taking place during warm working should be considered as a strain induced phenomenon.

The relationship between flow stresses and dynamic grain sizes evolved under warm deformation can be approximated by a power law equation, but it clearly differs from that for hot deformation (Fig. 7). The dynamic grains evolved under warm deformation are much finer than those expected from the extrapolated data under hot deformation. This suggests that any other nucleation mechanism can operate in grain interiors in addition to the bulging of grain boundaries.<sup>14)</sup> The same results for a warm-deformed copper are reported and discussed in detail elsewhere.<sup>14,25)</sup> The processes of fine grain evolution and the mechanisms operating in warm deformed copper are briefly summarised here. In the athermal region new grains can result from the evolution of deformation induced subboundaries with medium to high angle misorientations. This is considered, therefore, to be a kind of continuous reaction. The warm deformation brings about the formation of geometrically necessary dislocation subboundaries as dense dislocation walls, the misorientations of which increase with increase in strain. Subboundaries evolved faster near grain boundaries and slowly in grain interiors have middle to high angle misorientations at moderate strains and rapidly transform to grain boundaries of common type with further deformation, finally leading to the evolution of new fine grains at severe high strains.

The same discussions can be applied to the grain refinement taking place under warm multiple deformation of the present stainless steel. The  $\sigma$ - $\epsilon$  curves under warm deformation also suggest that the new grains are evolved by any other mechanism except conventional DRX, because the flow stresses in athermal region show no strain softening. Since static restorations hardly take place during interrupted deformation (see Fig. 2), strain-induced subboundaries are easily developed under multiple deformation because of strain accumulation and microstructural heterogeneities in previous deformation. The new grains can be rapidly evolved at appropriate places with high strain gradients, *e.g.* especially at grain boundary serrations and *etc.*<sup>14)</sup> The sequential change of loading direction (*i.e.* rotation of the samples) during multiple deformation also may play an important role in grain refinement.<sup>6,13)</sup>

It is concluded, therefore, that new grain evolution can result from continuous DRX under severe warm deformation at around  $0.5T_m$ . It is not yet entirely clear known how low angle subboundaries are transformed to high angle ones by multiple deformation, finally leading to the evolution of very fine grained structures. This new grain formation may be comparable with a dynamic recrystallization by progressive lattice rotations, namely subgrains developed along grain boundaries are progressively rotated accompanied by grain boundary sliding.<sup>11)</sup> The formation of new intergranu-

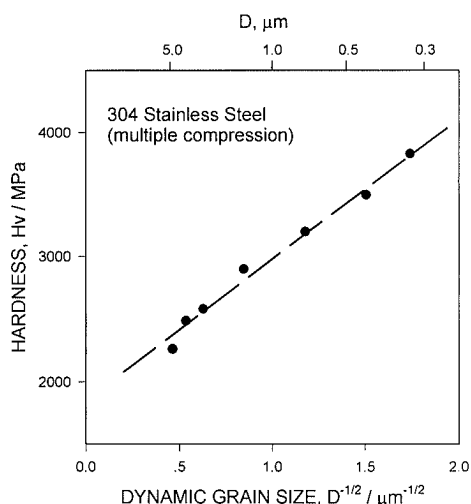


Fig. 11. Relationship between room temperature hardness ( $H_v$ ) and dynamic grain size ( $D$ ) evolved under multiple warm deformation.

lar interfaces as geometrically necessary subboundaries is considered as a structural response on the applied load under warm deformation condition. The present multiple deformation at hot to warm temperatures, therefore, provides a simple processing method for considerable grain refinement superior to usual DRX.

#### 4.3. Interrelation between Deformed Microstructures and Room-temperature Hardness

Figure 10 summarised the effect of microstructures (*i.e.* the volume fraction of new grains and average dislocation densities) evolved under single- and multi-pass compression on room-temperature hardness. Analysis of the experimental results revealed that the microstructural changes during deformation at  $T > 1023$  K (*i.e.* under hot working) are characterised by development of conventional DRX in both single- and multi-pass worked samples. On the other hand, microstructures evolved at  $T < 1023$  K (*i.e.* under warm working) depend on single or multi-pass testing method. Heterogeneous microstructures, composed of fine new grains with low dislocation densities and the part of original grains containing high density dislocations, are evolved under the latter deformation conditions (Figs. 6a, 6b). Relatively homogeneous substructures of high density dislocations, however, are developed in pan-caked original grains during single-pass compression.<sup>17)</sup> Note here, the dislocation densities in multiple deformed samples were averaged over the new grain interiors and the other work hardened regions.

It is clearly seen in Fig. 10c that the room-temperature hardnesses for the samples deformed by single- and multi-pass compression are close to each other in the region of hot working and so hardly depends on deformation history. On the other hand, the hardnesses for multiple deformation are higher than those for single-pass one at temperatures below 1023 K (*i.e.* under warm working conditions). It should be noted in Figs. 2 and 4 that the flow stresses developed under multiple deformation are almost similar to those under single-pass tests at temperatures below 1023 K.

The room-temperature hardnesses ( $H_v$ ) as well as the flow stresses in the region of athermal deformation can be generally related to the microstructural parameters, *e.g.* grain size ( $D$ ), with the same way,<sup>8,11,13,26)</sup> as shown in Fig. 11. The decrease in grain and/or subgrain size can lead to an increase in the hardness or the flow stress, while that in dislocation densities has an opposite effect. It can be concluded, thus, that the increase in hardness for multiple deformed samples is mainly associated with the new fine grains with high angle boundaries irrespective of the decrease in dislocation densities. An effect of grain refinement on the increase in room-temperature hardnesses (or flow stresses) can be bigger than that of decreasing of the dislocation densities. The former effect, however, decreases with temperature increasing and will be cancelled out by the latter one at warm temperatures. This can lead to the appearance of almost similar flow stresses at moderate strains under single and multiple warm deformation (Fig. 2).

#### 5. Conclusions

Dynamic processes of fine grain evolution and deformation behaviour under warm working conditions were studied by multiple compression of a 304 austenitic stainless steel with changing of the loading direction in  $90^\circ$  and with decreasing in deformation temperature from 1223 to 873 K ( $0.7-0.5T_m$ ) under a strain rate of  $8 \times 10^{-4} \text{ s}^{-1}$ , and the main results can be summarised as follows:

(1) There are two deformation regions where deformation characteristics are different. The deformation behaviours under flow stresses below around 400 MPa are typical for hot working conditions accompanied by conventional dynamic recrystallization (DRX).

(2) The relationship between grain size evolved under DRX and flow stress can be expressed by a power law function with a grain size exponent about  $-0.72$ . The DRX grains are nucleated by bulging of serrated grain boundaries assisted by strain induced subboundaries and twinning, *i.e.* discontinuous DRX.

(3) The deformation behaviours under flow stresses above 400 MPa hardly depend on strain rate and temperature and so are in the region of athermal deformation. The stress-strain curves show steady-state-like flows without any strain softening irrespective of the development of new fine grains with high angle misorientations.

(4) The average sizes of new fine grains below  $1 \mu\text{m}$  developed under warm working conditions can be also related to the flow stresses through another power law function with a grain size exponent about  $-0.42$ . The dynamic evolution of fine grains results from continuous reactions, *i.e.* the evolution of deformation induced dislocation subboundaries, the misorientations of which increase with increase in strain, finally leading to the evolution of new fine grains, *i.e.* continuous DRX.

(5) The room-temperature hardnesses after multiple warm working are higher than those for single-pass one, although warm temperature flow stresses are almost

similar in the both deformation modes. The increase in hardness is mainly associated with the new fine grains irrespective of the decrease in dislocation densities in them.

#### Acknowledgements

The authors acknowledge with gratitude the financial support received from the Recrystallization and Texture Committee of the Iron and Steel Institute of Japan. They also wish to thank NKK Co. Ltd., for supplying the test material. One of authors (A.B.) also would like to express his hearty thanks to the Japan Society for the Promotion of Science and the University of Electro-Communications for providing scientific fellowships.

#### REFERENCES

- 1) N. A. Smirnova, V. I. Levit, V. I. Pilyugin, R. I. Kuznetsov, L. S. Davydova and V. A. Sazonova: *Phys. Met. Metallogr.*, **61** (1986), 127.
- 2) R. Z. Valiev: *Ann. Chim. Fr.*, **21** (1996), 369.
- 3) R. Z. Valiev, Yu. V. Ivanisenko, E. F. Rauch and B. Baudelet: *Acta Metall.*, **44** (1996), 4705.
- 4) A. Belyakov, R. Kaibyshev and T. Sakai: Interface Science and Materials Interconnection (iib'96, JIMIS-8), ed. by Y. Ishida *et al.*, JIM, (1996), 495.
- 5) G. A. Salishchev, R. G. Zaripova, A. A. Zakirova and H. J. McQueen: Hot Workability of Steels and Light Alloys-Composites, ed. by H. J. McQueen *et al.*, TMS-CIM, Montreal, (1996), 217.
- 6) Y. Iwahashi, Z. Horita, M. Nemoto and T. G. Langdon: *Acta Mater.*, **45** (1997), 4733.
- 7) R. Kaibyshev and O. Sitdikov: *Z. Metallkd.*, **85** (1994), 738.
- 8) H. J. McQueen and J. J. Jonas: Treatise on Materials Science and Technology, ed. by R. J. Arsenault, Academic Press, (1975), 393.
- 9) T. Sakai and J. J. Jonas: *Acta Metall.*, **32** (1984), 189.
- 10) T. Sakai: *J. Mater. Process. Technol.*, **53** (1995), 349.
- 11) F. J. Humphreys and M. Hatherly: Recrystallization and Related Annealing Phenomena, Pergamon Press, Oxford, (1996), 363.
- 12) A. Belyakov, R. Kaibyshev and T. Sakai: *Metall. Trans. A*, **29A** (1998), 161.
- 13) T. Hayashi, O. Umezawa, S. Toritsuka, T. Mitsui, K. Tsuzaki and H. Nagai: *CAMP-ISIJ*, **11** (1998), 1031.
- 14) A. Belyakov, W. Gao, H. Miura and T. Sakai: *Metall. Trans. A*, **29A** (1998), 2957.
- 15) T. Maki, T. Akasaka, K. Okuno and I. Tamura: *Trans. Iron Steel Jpn.*, **22** (1982), 253.
- 16) N. D. Ryan and H. J. McQueen, *Can. Metall. Q.*, **29** (1990), 147.
- 17) A. Belyakov, H. Miura and T. Sakai: *Mater. Sci. Eng.*, **A255** (1998), 139.
- 18) E. Inoue and T. Sakai: *J. Jpn. Inst. Met.*, **55** (1991), 286.
- 19) G. Tomas and M. J. Goringe: Transmission Electron Microscopy of Materials, Wiley, New York, (1979), 112.
- 20) T. Sakai, M. G. Akben and J. J. Jonas: *Acta Metall.*, **31** (1983), 631.
- 21) B. Bay, N. Hansen, D. A. Hughes and D. Kuhlmann-Wilsdorf: *Acta Metall. Mater.*, **40** (1992), 205.
- 22) D. A. Hughes, Q. Liu, D. C. Chrzan and N. Hansen: *Acta Mater.*, **45** (1997), 105.
- 23) T. Sakai and M. Ohashi: *Mater. Sci. Tech.*, **6** (1990), 1251.
- 24) H. Miura, H. Aoyama and T. Sakai, *J. Jpn. Inst. Met.*, **58** (1994), 269.
- 25) A. Belyakov, H. Miura and T. Sakai: *ISIJ Int.*, **38** (1998), 595.
- 26) M. Furukawa, Z. Horita, M. Nemoto, R. Valiev and T. Langdon: *Phil. Mag. A*, **78** (1998), 203.